RESEARCH ARTICLE

Proteomics Profiling of Host Cell Response via Protein Expression and Phosphorylation upon Dengue Virus Infection

Meng Miao[1] · Fei Yu[1,2] · Danya Wang[1,2] · Yongjia Tong[1,2] · Liuting Yang[1,2] · Jiuyue Xu[3] · Yang Qiu[3] ·
Xi Zhou[1,3] 🔟 · Xiaolu Zhao[1,2] 🔟

Abstract

Dengue virus (DENV) infection is a worldwide public health threat. To date, the knowledge about the pathogenesis and progression of DENV infection is still limited. Combining global profiling based on proteomic analysis together with functional verification analysis is a powerful strategy to investigate the interplay between the virus and host cells. In the present study, quantitative proteomics has been applied to evaluate host responses (as indicated by altered proteins and modifications) in human cells (using K562 cell line) upon DENV-2 infection, as DENV-2 spreads most widely among all DENV serotypes. Comparative analysis was performed to define differentially expressed proteins in the infected cells compared to the mock-control, and it revealed critical pathogen-induced changes covering a broad spectrum of host cellular compartments and processes. We also discovered more dramatic changes (> 20%, 160 regulated phosphoproteins) in protein phosphorylation compared to protein expression (14%, 321 regulated proteins). Most of these proteins/phosphoproteins were involved in transcription regulation, RNA splicing and processing, immune system, cellular response to stimulus, and macromolecule biosynthesis. Western blot analysis was also performed to confirm the proteomic data. Potential roles of these altered proteins were discussed. The present study provides valuable large-scale protein-related information for elucidating the functional emphasis of host cell proteins and their post-translational modifications in virus infection, and also provides insight and protein evidence for understanding the general pathogenesis and pathology of DENV.

✉ Xi Zhou
zhouxi@whu.edu.cn

✉ Xiaolu Zhao
zhaoxiaolu@whu.edu.cn

1   State Key Laboratory of Virology, College of Life Sciences, Wuhan University, Wuhan 430072, China

2   Hubei Key Laboratory of Cell Homeostasis, College of Life Sciences, Wuhan University, Wuhan 430072, China

3   Laboratory of RNA Virology, Wuhan Institute of Virology, Chinese Academy of Science, Wuhan 430071, China

Introduction

Dengue virus (DENV) belongs to the genus *Flavivirus* in the family *Flaviviridae*, which is a large group of single-stranded, positive-sense RNA viruses [(+)ssRNA] with a genome of approximately 10.7 kb in length. Since the discovery of DENV in 1943 (Messina *et al.* 2014), the reported incidence of these infections has increased in tropical and subtropical areas of the world, and it has recently caused local outbreaks in China, America, Australia, France and many other countries (Zhao *et al.* 2016; Li *et al.* 2017; Radke *et al.* 2012; Bhatt *et al.* 2013; Schaffner *et al.* 2014; WHO 2019).

In 2011, the WHO revised its classifications and now grades the disease severity by its clinical manifestations as dengue fever (DF) and dengue hemorrhagic fever (DHF) grades 1–4. Currently, there are four distinct, but closely

related serotypes of DENV (DENV1–4). These four serotypes are genetically similar and share approximately 65% of their genomes, among them DENV-2 spreads most widely. All of these DENV serotypes are transmitted to humans principally by two mosquito vectors, *Aedes aegypti* and *Aedes albopictus*, and cause a wide range of symptoms from a flu-like DF to more severe and even fatal DHFs (Simmons *et al.* 2012).

The linear (+)ssRNA genome of DENV contains a single open reading frame (ORF), encoding the polyprotein with a $5'$ type-I m^7G cap structure. The polyprotein is post-translationally cleaved by host- or viral proteases to produce separate structural (C, prM/M, E) and nonstructural (NS1-NS2A-NS2B-NS3-NS4A-NS4B-NS5) proteins (Green *et al.* 2014).

The DENV virion enters target cells via receptor mediated endocytosis in a clathrin-dependent manner (Savidis *et al.* 2016; Acosta *et al.* 2008). After the initial translation and cleavage of the polyprotein, DENV triggers the formation of a replication complex in the perinuclear endoplasmic reticulum, where RNA replication and protein translation occur. The newly synthesized positive-sense viral RNA is then packaged by the C protein and assembled into an enveloped virion that is covered with prM/E heterodimers (Welsch *et al.* 2009). The mature virus particles released by exocytosis can infect other cells.

The genome of DENV is relatively small in size and simple in composition compared to host eukaryotic genomes. And the ten proteins encoded by DENV are insufficient for viral life cycle. Like other viruses, DENV has evolved many strategies to hijack and utilize host factors throughout its life cycle. It has been reported that the NS5 proteins of many flaviviruses, including DENV, West Niles virus, Japanese Encephalitis virus, Zika virus, and Yellow Fever virus, possess $2'$-O-methyltransferase activity to modify the $5'$ cap structure of viral mRNAs, thereby mimicking eukaryotic type 1 cap structures and competing for eIF4e binding (Daffis *et al.* 2010). The DENV NS2B/3 protease can cleave STING, thereby preventing type I interferon (IFN) induction mediated by cGAS (Aguirre *et al.* 2012).

Upon viral infection, the host cells mobilize a coordinated response. Proteomics analysis has been proven to be an effective approach to obtain a global and quantitative assessment of host-virus interactions, and has widely been used in studies of many important viruses (Xin *et al.* 2017; Clements *et al.* 2017; Ersing *et al.* 2017; Weekes *et al.* 2014). Mass spectrometry-based quantitative proteomics is an efficient tool for gene selection and can provide an insight in regulated biological processes on functional level. Bottom-up proteomics strategy is most popular, in which peptides are measured as surrogates for the protein of interest (Schubert *et al.* 2017) and stable isotopic

labeling based quantification methods are usually employed for peptide/protein quantitation. Dimethyl-labeling is a simple, robust, and reliable multiplex labeling method and has been widely applied to quantitative proteomics (Hsu and Chen 2016).

In this study, we have determined changes in the host cell protein expression and protein phosphorylation during uptake of DENV using dimethyl-labeling based quantitative proteomics. A total of 2263 host proteins and 2440 phosphorylated sites on 799 host phosphoproteins were quantified, of which around 14% of proteins and 20% phosphoproteins showed significantly regulation, covering a broad spectrum of cellular compartments and biological pathways. Our study revealed critical pathogen-induced changes in host protein expression and protein phosphorylation and further unveiled vital changes in cellular processes as response to DENV infection.

Materials and Methods

Cultivation of K562 Cells and Dengue Virus Production and Stock

Human erythroleukemic K562 cells were maintained in RPMI 1640 medium (Invitrogen) supplemented with 10% FBS (GIBCO) at 37 °C in 5% CO_2. C6/36 (*Ae. Albopictus* epithelial cells) cells were cultured in RPMI 1640 medium supplemented with 10% FBS, 100 U/mL of L-glutamine, 100 mg/mL of penicillin–streptomycin and maintained at 28 °C.

DENV-2 strain TSV01 was used in this study. Monolayers of C6/36 cells were infected with DENV-2 at a multiplicity of infection (MOI) of 0.01, and 6 days after infection, cell supernatants were collected, clarified, and stored at − 80 °C. The titers of DENV-2 stocks were determined by limiting-dilution plaque assay on BHK cells.

Infection of K562 Cells with Dengue Virus

Human erythroleukemic K562 cells were maintained as described above, and at day 2 of culture, samples of 1×10^7 cells were resuspended in RPMI 1640 medium supplemented with 2% FBS and were infected with the DENV-2 at the MOI of 10. The DENV-2 infection level in K562 cells was measured by qRT-PCR analysis. Total RNA was purified using TRIzol reagent (Thermo) according to the manufacturer's protocol. qRT-PCR was performed on a StepOne Real-Time PCR Systerm with SYBR qPCR Mix (TOYOBO). The primers were F: GCAGAAACACAACAT GGAACAATAGT, R: TGATGTAGCTGTCTCCGAATGG.

Protein Extraction and Digestion

The pellet of cells infected with DENV-2 was resuspended in 200 μL of lysis buffer containing 6 mol/L urea, 2 mol/L thiourea, 5 mmol/L DTT, 1 mmol/L NaF, 0.2 mmol/L NaVO$_3$, 1 mmol/L EDTA, 0.5 mmol/L EGTA, Complete protease inhibitor cocktail and PhosStop phosphatase inhibitor cocktail (Roche), pH 8.0. After sonication for 3 min (5-s intervals for every 2-s sonication) on ice, sonicated lysate was centrifuged at 20,000 $\times g$ for 20 min. The protein concentration was determined by the Bradford assay. The protein solution was reduced with DTT (5 mmol/L) at 37 °C for 45 min, alkylated with iodoacetamide (15 mmol/L) at room temperature for 45 min, and then digested with Lys-C (1:30) at room temperature for 4 h. After sixfold dilution with H$_2$O, the solution was subsequently digested overnight with trypsin (1:50) at 37 °C.

On-column Desalting and Dimethyl Labelling

On-column desalting and dimethyl labelling was performed as previously described with minor modifications (Boersema *et al.* 2009). P100 microcolumns were packed with the POROS OLIGOR3 reversed phase resin (20 μm; Applied Biosystems). The length of microcolumns was made according to the sample amount (1 cm for 100 μg). The columns were equilibrated with 0.1% TFA. Samples were loaded onto the columns in 50 μL of 0.1% TFA and washed twice with 100 μL of 0.1% TFA. The column was flushed slowly with 100 μL of the respective labeling reagent (light, intermediate) five times, washed with 100 μL of H$_2$O twice, eluted with 100 μL of 50% acetonitrile (ACN) and 100 μL of 70% ACN. The differentially labeled samples were mixed, lyophilized and stored at − 80 °C for later HILIC fractionation.

TiO$_2$ Enrichment of Phosphopeptides

Phosphopeptides were enriched by TiO$_2$ as previously described (Zhao *et al.* 2014). The 200 μg digested peptides was re-suspended in 200 μL loading buffer (80% ACN, 5% TFA, 1 mol/L glycolic acid) and mixed with TiO$_2$ material in the Eppendorf tube for 10 min. The resin was first washed with loading buffer and sequentially washed with three washing buffers (80% ACN/1% TFA, 20% ACN/0.1% TFA, and water). The phosphopeptides were eluted by mixing the resins with NH$_3$·H$_2$O (pH 10.5) for incubation in 10 min. The elution was acidified with 100% formic acid and desalted using a R3 microcolumn prior to further fractionation by HILIC.

Hydrophilic Interaction Liquid Chromatography (HILIC) Fractionation

The peptides were fractionated by HILIC. Chromatographic separations were performed on an Agilent 1200 Series HPLC system (Agilent) using a custom-made 320 μm × 180 mm HILIC column packed with TSKGel Amide-80 3 μm HILIC particles (Tosoh Biosciences). The dried peptides were resuspended and loaded in Solvent B (90% ACN, 0.1% TFA) onto a HILIC column at a flow rate of 12 μL/min in 8.5 min. The peptides were separated by an inverse gradient of 100%–90% Solvent B in 0.5 min, 90%–60% Solvent B in 26 min, followed by 60%–0% Solvent B in 4 min with an increasing amount of Solvent A (0.1% TFA) at a flow rate of 6 μL/min. A total of 36 fractions were collected throughout the gradient, pooled into eight fractions and lyophilized down in a vacuum centrifuge for later LC–MS/MS analysis.

LC–MS/MS Analysis

LC–MS/MS analysis were performed using an EasyLC system (Thermo Scientific, Odense, DK) interfaced to an LTQ-Orbitrap XL hybrid mass spectrometer (ThermoFisher, Bremen, Germany) as previously described. Samples were dissolved in Solvent A (0.5% FA) and loaded at a flow rate of 550 nL/min onto a custom-made 16-cm analytical column [100-m inner diameter, 375-m outer diameter, packed with Reprosil C18, 3 μm reversed phase particles (Dr. Maisch GmbH)]. Separation was then performed at a flow rate of 250 nL/min using a 100-min gradient of 0%–34% Solvent B (90% ACN, 0.5% FA). The LTQ-Orbitrap XL instrument was operated in a data-dependent MS/MS mode. Multistage activation (MSA) was used for phosphorylated peptides. Full scans were acquired in the Orbitrap, and up to five of the most intense peptides were selected and subjected to fragmentation in the linear ion trap (LTQ).

Database Search and Data Interpretation

The LC–MS/MS data were processed and searched against Uniprot Homo sapiens protein sequence database (retrieved on 20,205 sequences) using MaxQuant (Version 1.5.2.8) for protein identification and quantification. Trypsin was chosen as the enzyme with a maximum of two missed cleavages allowed. S-Carbamidomethyl cysteine and demethylation (N-terminal and lysine) were defined as a fixed modification. Partial modifications included were oxidation (M) and phosphorylation at serine, threonine, and tyrosine residues. The MS and MS/MS results were searched with a peptide ion mass tolerance of 10 ppm and a fragment ion mass tolerance of 0.6 Da. Proteins were

identified with a confidence score of > 95. The false discovery rate (FDR) calculated based on a decoy database search was set to 1%. Gaussian distributions of ratios were analyzed and mean $\pm$ 1.96 SD was used as the cut-off for significant regulations.

Bioinformatics

Gene ontology (GO) analysis and functional classification were performed by using Panther (Version11.0) (Mi *et al.* 2017). The Biological Networks Gene Ontology (BiNGO, Version 3.0.3) (Maere *et al.* 2005) plug-in implemented in the Cytoscape (http://www.cytoscape.org/, Version 3.6.1) (Shannon *et al.* 2003) was used to analyze the GO term enrichment of significantly up- or down-regulated proteins ($P < 0.001$, statistical test by Hypergeometric test). STRING (the Search Tool for the Retrieval of Interacting Genes/Proteins, Version 10.5) (Szklarczyk *et al.* 2017) was utilized to qualify the physical and functional protein–protein interactions, which were then visualized in Cytoscape.

Western Blot

Infection of K562 cells was performed as described above. Cells were harvested in cell lysis buffer [50 mmol/L Tris–HCl (pH 7.4), 150 mmol/L NaCl, 1% NP40, 0.25% deoxycholate and a protease inhibitor cocktail (Roche)]. Crude lysates were boiled for 10 min and then kept on ice. Each sample was loaded in a 12% polyacrylamide-SDS gel, and the proteins were electrophoretically separated by conventional methods. Proteins were transferred to nitrocellulose, and blots were incubated with anti-Tubulin (Proteintech), rabbit monoclonal antibodies anti-SAP18, rabbit monoclonal antibodies anti-GRB2, rabbit monoclonal antibodies anti- eIF3e, rabbit monoclonal antibodies anti-Bid, rabbit monoclonal antibodies anti-HDAC1 (Abcam).

Results

Proteomics Analysis of Host Proteins upon DENV Infection

DENV infection affects various host cellular pathways including interferon responses, apoptosis and endoplasmic reticulum stress. Knowledge of changes in host protein expression and phosphorylation caused by infection helps to understand the interaction between virus infection and host response. In this study, a dimethyl labelling-based quantitative proteomics strategy was employed to characterize the host cell proteome and phospho-proteome

changes upon DENV infection in K562 cells (Fig. 1A). Briefly, K562 cells were infected with DENV-2 at a multiplicity of infection (MOI) of 10 or mock treated and were harvested and lysed at 48 h post infection (hpi). The DENV-2 infected K562 cells were analyzed by qRT-PCR (Fig. 1B). Extracted proteins were tryptic digested, and the digested peptides from mock-treated or DENV-infected cells were differentially labeled with light or medium dimethyl reagent, respectively. The labeled peptides were mixed in a ratio of 1:1, subjected to TiO_2 phospho-enrichment, offlinely fractionated by hydrophilic interaction liquid chromatography (HILIC), and then analyzed by liquid chromatography-tandem mass spectrometry (LC–MS/MS) (Fig. 1A). Three independent biological replicates were performed.

MS data were submitted to Maxquant to perform peptide identification and quantitation. Using these criteria that only proteins with at least two quantified peptides with a confidence score of > 95 were quantified, a total of 2263 host proteins and 2440 phosphorylated sites on 799 host phosphoproteins were identified (Table 1 and Fig. 1C). The cutoff for differentially regulated proteins was set as described previously (Xin *et al.* 2017). Briefly, the Gaussian distribution of protein ratios was analyzed, and proteins with ratios deviating from the mean of the normally distributed data by 1.96 standard deviations (SDs) were considered differentially regulated (Supplementary Figure S1). Using this criterion, we found that 201 proteins were identified as being upregulated, while 120 were identified as being downregulated out of the 2263 quantified host proteins. And 103/85 phosphoproteins were identified as being upregulated/downregulated, while 301/200 phosphosites were identified as being upregulated/downregulated out of the 2440 quantified phosphosites among the 799 host phosphoprotein (Table 1) (detail information in Supplementary Table S1–S3). As indicated in Fig. 1C, 14.1% of all quantified proteins were significantly regulated, whereas higher percentages (23.4%/20.4%) of all quantified phospho-proteins/sites showed significant regulation, implying a bigger effect on host protein phosphorylation caused by DENV infection as compared to protein expression. Interestingly, relatively higher numbers of upregulation in expression and phosphorylation were observed for the same host proteins (Fig. 1C).

Functional Classification of Regulated Protein/ Phosphoproteins in Response to DENV Infection

Gene ontology (GO) descriptions were referred to their annotations in the NCBI database. To obtain an overview of functional classification of all the differentially regulated proteins, the 201 upregulated and 120 downregulated
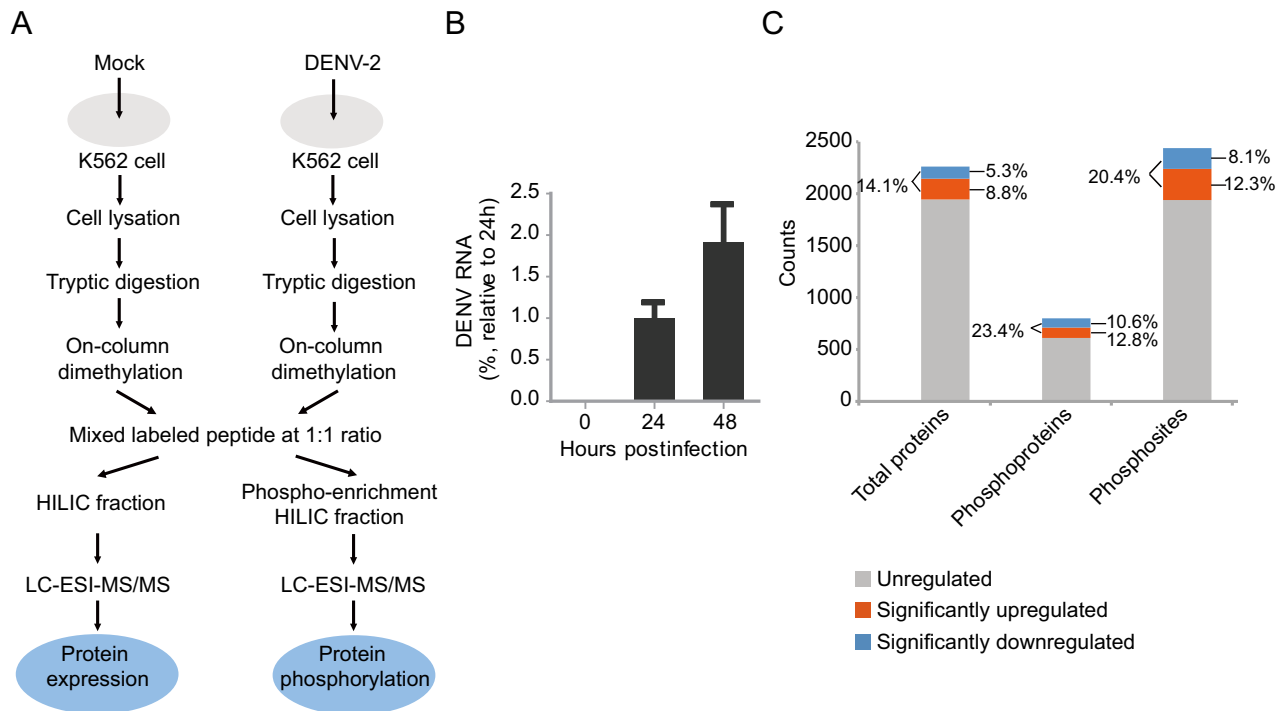
Fig. 1 Proteomics and phosphoproteomics profiling of DENV-2 infection in human K562 cells. **A** Workflow for quantitative proteomic analysis of DENV-2 infected K562 cells. **B** qRT-PCR analysis of DENV-2 levels in K562 cells. K562 cells were infected with DENV-2 strains TSV01 at a MOI of 10. The intracellular DENV-2 RNA was extracted and measured by qRT-PCR at different time points. Three independent biological replicates were performed. **C** An overview of all identified and regulated proteins, phosphoproteins and phosphosites. Orange box represented upregulated protein/phosphosite, blue box represented downregulated protein/phosphosite, gray box represented unregulated protein/phosphosite.

Table 1 An overview of proteins, phosphoproteins and phosphosites quantified in this study.

	Biological replicate 1	Biological replicate 2	Biological replicate 3	Total
Total protein				
Unregulated	1775	1845	1771	1942
Significantly upregulated	83	68	98	201
Significantly downregulated	57	72	60	120
Phosphoproteins				
Unregulated	549	622	617	611
Significantly upregulated	53	49	41	103
Significantly downregulated	28	38	55	85
Phosphosites				
Unregulated	1563	1840	1947	1939
Significantly upregulated	178	124	70	301
Significantly downregulated	107	79	64	200

In total, 2263 proteins, 799 phosphoproteins and 2440 phosphosites were quantified. Gaussian distribution (mean $\pm$ 1.96SD) was applied to filter out the significantly regulated proteins/sites.

proteins together with 103 upregulated and 85 downregulated phosphoproteins were submitted to Panther for GO analysis. The results showed that the regulated proteins appeared to be involved in a broad range of cellular biological processes and categorized into ten to twelve functional groups (Fig. 2A–2D) (detail information in Supplementary Table S4). Obviously, a broad spectrum of host proteins/phosphoproteins was involved in virus

infection and host response with similar pattern of functional classification. The three largest groups of regulated proteins were identified involving in metabolic process, cellular process, and cellular component organization or biogenesis, composing high variety of proteins with vital cellular functions. In addition, a smaller quantity of the regulated proteins/phosphoproteins involved in response to stimulus and immune system process was found. Moreover, for both proteins and phosphoproteins, upregulated proteins exhibited different patterns as compared to downregulated proteins in most processes except for the three major processes. Especially, higher percentage of upregulated proteins was distributed in response to stimulus than downregulated proteins (Fig. 2A–2D, words highlighted in red). High similarity was shared between protein expression and phosphorylation in response to DENV infection.

To assess the statistical overrepresentation of specific categories of regulated proteins relative to all quantified proteins, a hypergeometric test in GO annotation was performed by using BinGo. Such statistical enrichment analysis can assess whether the numeric values of proteins in certain biological processes are nonrandomly distributed with respect to the numeric values of all quantified proteins. Categories with normalized $P < 0.001$ were considered overrepresented. As illustrated in Fig. 3A (detail

Fig. 3 GO analysis of regulated protein and phosphoprotein. List of ▶ regulated total proteins and phosphoproteins were submitted to BINGO to perform a GO enrichment analysis. **A** Go analysis of regulated total proteins ($P < 0.001$). **B** GO analysis of regulated phosphoproteins ($P < 0.001$). Whole annotation is as reference. Area of circles represents included gene numbers. $P < 0.001$ defines over-represent categories. Green line represents "Cellular macromolecule biosynthetic process". Purple line represents "RNA splicing". Blue line represents "mRNA processing". Black line represents "Regulation of transcription".

information in Supplementary Table S5), the distributions of proteins in the categories—macromolecule biosynthetic process, RNA splicing, Golgi vesicle transport and cellular membrane organization were identified as highly overrepresented in total proteins, suggesting that these biological processes were activated by DENV infection (Fig. 3A). In comparison, the distributions of phosphoproteins in the biological processes including negative regulation of nucleobase, nucleoside, nucleotide and nucleic acid metabolic process, negative regulation of gene expression, chromatin modification, macromolecular complex assembly, RNA splicing, cell cycle, mRNA Processing and regulation of transcription were significantly higher than the overall distribution, implying that these processes were highly regulated by reversible protein phosphorylation in
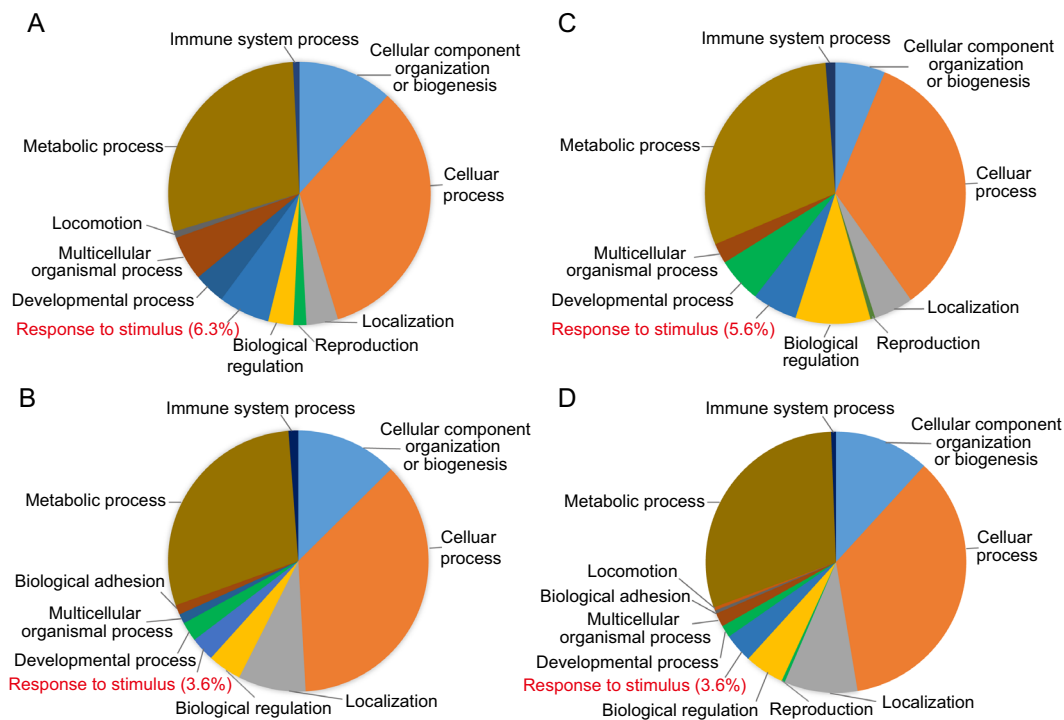

Fig. 2 Functional classification analysis. List of regulated total proteins and phosphoproteins were submitted to PANTHER to perform a gene classification analysis. **A** Upregulated total proteins, **B** downregulated total proteins, **C** upregulated phosphoproteins, **D** downregulated phosphoproteins. Different colors represent different biological processes; area of fans represent the number of included proteins. "response to stimulus" was highlighted in red.
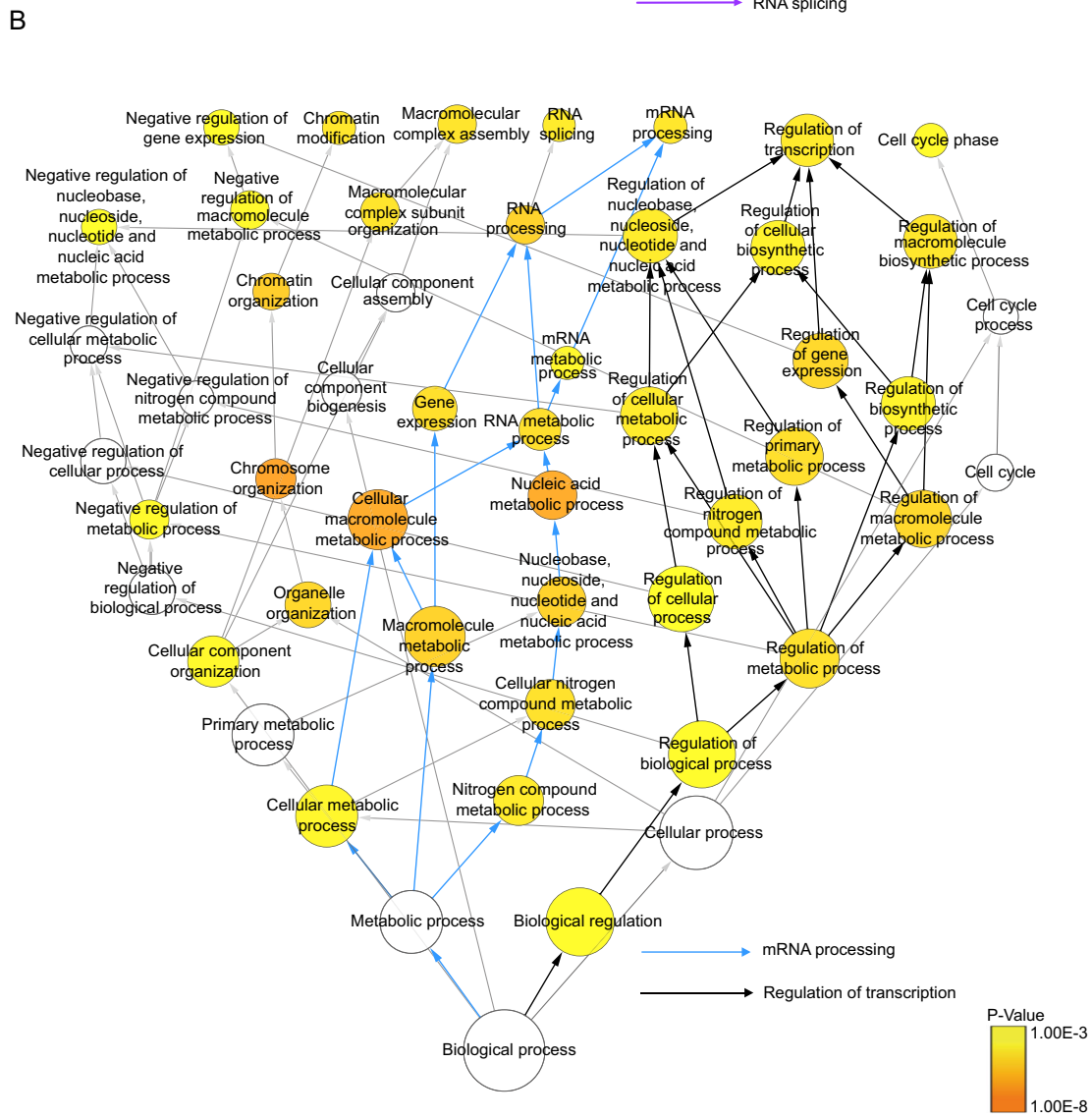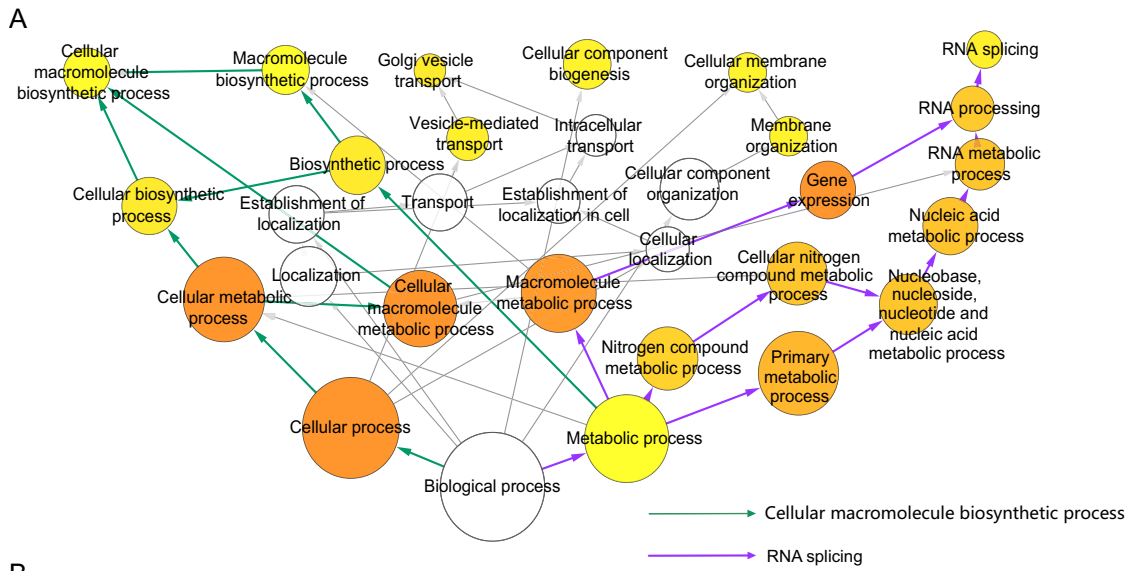
virus and host interaction (Fig. 3B). Nucleic acid metabolic process was enriched for both regulated proteins and phosphoproteins emphasizing its role in response to DENV infection.

To better understand the host cellular response to DENV infection, annotations of all regulated proteins were examined manually. We found that the majority of regulated proteins were involved in RNA splicing and cellular macromolecule biosynthetic process. These two processes were found to be the two most overrepresented processes upon DENV infection with a low P values (highlighted in purple and green arrows, respectively in Fig. 3A). For protein phosphorylation, mRNA processing and transcriptional regulation were found to be the two most overrepresented processes in response to DENV infection (highlighted in blue and black arrows, respectively in Fig. 3B).

Protein–Protein Interaction Analysis of Most Overrepresented Processes in Response to DENV Infection

To explore potential protein network connections for the significantly enriched processes from GO analysis, the regulated proteins involved in the most enriched pathways were analyzed by using STRING in which the interactions were documented according to known and predicted protein–protein interactions. The resulting protein networks were visualized in Cytoscape (Fig. 4, detail information in Supplementary Table S6).

For protein expression, proteins involved in RNA splicing and cellular macromolecule biosynthetic process were of great interests and chosen for protein–protein interaction analysis. A highly interacting protein network was formed, consisting of 54 individual proteins and 195 distinct interactions (Fig. 4A). Proteins interact not only with proteins involved in the same process but also with proteins in the other process. RNA splicing and cellular macromolecule biosynthetic process were represented in rectangle and ellipse, respectively, with diamond representing the overlap. Up/down-regulation information was also included and highlighted in red/blue for clear comparison. As showed in Fig. 4A, more proteins were found to be upregulated than downregulated in both processes.

Those proteins which showed regulated expression by virus infection and appeared to actively interact with other proteins might be the key players in the antiviral response. Based on our MS results and the protein–protein interaction analysis as well as previous knowledge, several proteins drew our attention, which were EIF3E, BID, HDAC1, GRB2, and SAP18. They were all upregulated upon DENV infection revealed by mass spectrometric analysis and were

highly interacting with proteins involved in cellular macromolecule biosynthetic process (Fig. 4A).

EIF3E is the component of the eukaryotic translation initiation factor 3 (eIF-3) complex, which is required for several steps in the initiation of protein synthesis (Masutani *et al.* 2007). EIF3E has been reported as a binding partner of classical swine fever virus (CSFV) NS5A protein. Overexpression of EIF3E markedly enhanced CSFV genomic RNA replication, viral protein expression and production of progeny virus (Liu *et al.* 2018). BID is a proapoptotic Bcl-2 protein containing only the BH3 domain (Wang *et al.* 1996). BID interacts with BAX, leading to the insertion of BAX into organelle membranes and finally induces apoptosis. Although apoptosis has been detected *in vivo* and *in vitro* in response to DENV infection, the mechanism is not completely understood (Thongtan *et al.* 2004). In our work, BID was 1.7 fold higher in abundance after infection. It may be involved in DENV-induced apoptosis and was worthy for further investigation. GRB2 (Growth factor receptor-bound protein 2) is an adapter protein that provides a critical link between cell surface growth factor receptors and the Ras signaling pathway. It has been reported that HCV NS5A can specifically interacts with GRB2 and inhibits the MAPK/ERK pathway (Huynh *et al.* 2016). SAP18 (Sin3a-associated protein of 18 kDa) is a component of the SIN3-HDAC1 complex which can direct the formation of a repressive complex to core histone proteins and induce transcriptional repression (Zhang *et al.* 1997). SAP18 was also found to be correlated with RNA splicing (Singh *et al.* 2010). One work has find that HIV-1 IN protein can specifically interact with SAP18 and recruit the Sin3a-HDAC1 complex into HIV-1 virion. The deacetylase activity is important for the subsequent stages of viral replication (Sorin *et al.* 2009).

To verify our MS data, Western blotting analysis of selected host proteins was performed. As shown in Fig. 4B, Western blotting data showed that the proteins EIF3E, BID, HDAC1, GRB and SAP18 were upregulated as a result of DENV infection (Fig. 4B), consistent with our MS data.

For protein phosphorylation, phosphoproteins which were significantly regulated upon infection and involved in mRNA processing and regulation of transcription were also further looked into for protein–protein interaction analysis. A network consisting of highly interacting 48 phosphoproteins was formed and 133 distinct interactions between phospho-proteins in the same process and in the other process were illustrated in Fig. 4C. Equal number of upregulated and downregulated phosphoproteins was found to be involved in both processes.

Our data set provides a source of phospho-peptide sequences for exploring the network between different kinase families and their substrates. NetworKIN was used
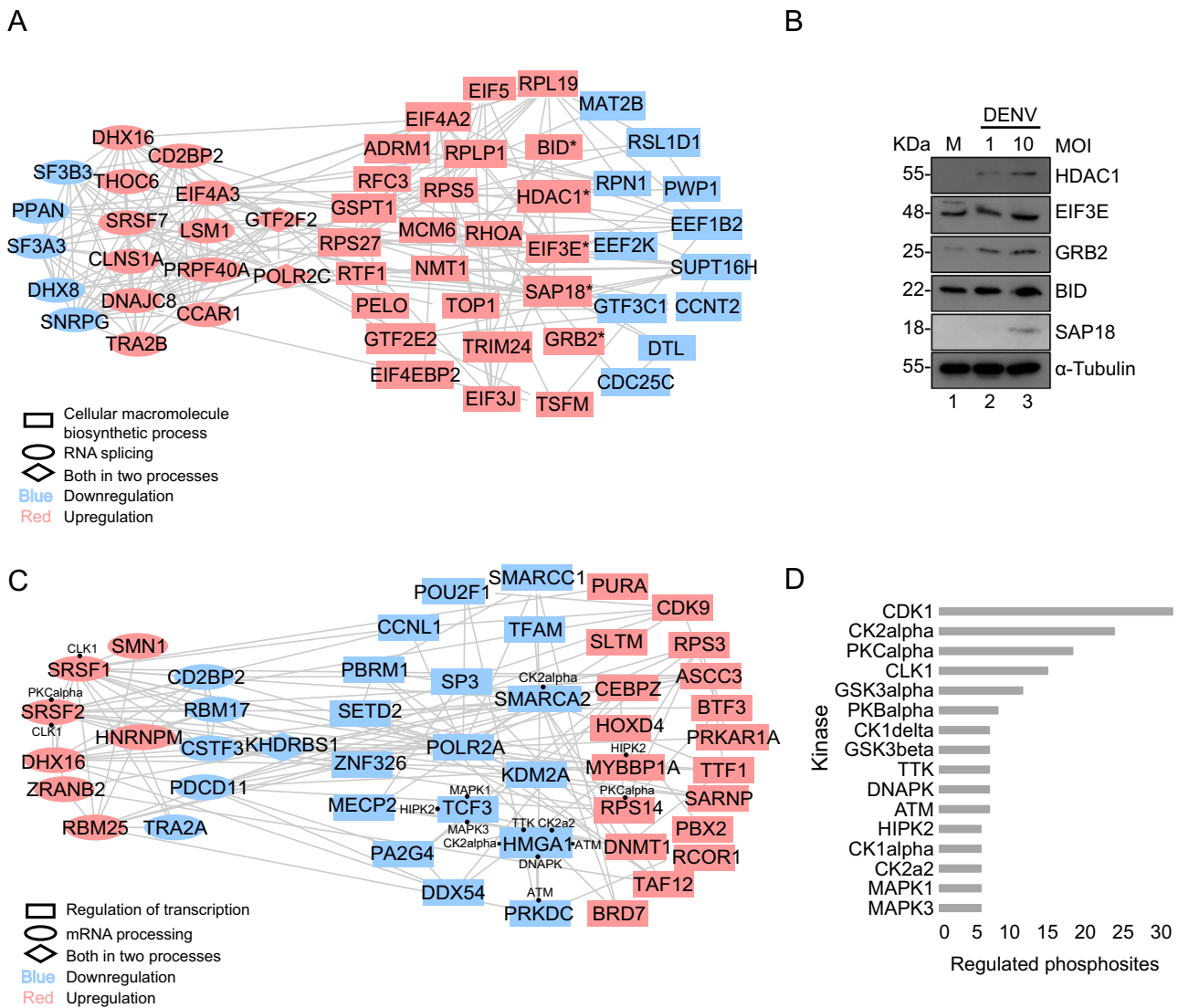
A

B

C

D

Fig. 4 Protein–protein interaction network of regulated protein. List of "Cellular macromolecule biosynthetic process" and "RNA splicing" among total protein, "mRNA processing" and "Regulation of gene expression" among phosphoprotein were submitted to STRING to perform an interaction analysis and visualized by Cytoscape. **A** Network of "Cellular macromolecule biosynthetic process" and "RNA splicing" from regulated total proteins. The network includes 54 nodes (proteins) and 195 edges (interactions). Asterisk represents interested proteins. **B** Western blot validation of 5 interested genes. **C** Network of "mRNA processing" and "Regulation of gene expression" from regulated phosphoproteins. The network includes 48 nodes (proteins) and 133 edges (interactions). Black dot represents interacted predicted kinases. **D** Kinase prediction of regulated phosphoproteins.

to generate a list of predicted potential kinases for the regulated phosphorylation sites. Prediction was based on comparison of the phosphorylation sites with reported consensus sequences for different protein kinases. The number of distinct phosphorylation sites for each kinase family was illustrated in Fig. 4D (detailed information in Supplementary Table S7. The kinase prediction of identified phosphorylation sites exhibited a broad range of kinase families which might target various host proteins in the process of virus infection. It suggests major role for the CDK1, CK2alpha, PKCalpha, CLK1, GSK3alpha and PKBalpha kinase families, implicating the greatest

proportion of the identified distinct phosphorylation sites are their potential substrates. As marked in Fig. 4C, several upregulated proteins involved in both mRNA processing and regulation of transcription, as well as more downregulated proteins involved in regulation of transcription were found to be the substrates of those major kinase families.

Discussion

This is the first large-scale systematic quantitative proteomics and phosphoproteomics analysis of DENV-infected host cells. The expression patterns of 2263 host proteins were profiled, among which 321 were differentially regulated as a result of DENV infection. The phosphorylation levels of 2440 phosphorylated sites located in 799 phosphoproteins were investigated, among which 501 phosphorylation sites in 188 phosphoproteins showed regulated levels upon infection. To better understand the cellular response to DENV infection in K562 cells, a global map was created in which regulated host proteins/phosphoproteins are categorized according to their functions and cellular compartments (Fig. 5). The highest numbers of regulated proteins and phosphoproteins were found to be related to cellular macromolecule biosynthetic process, RNA splicing, chromatin modification and response to stimulus.

The viral RNA replication of DENV is dependent on intracellular membrane system. The initial infection of DENV is mediated by clathrin-dependent receptor-mediated endocytosis. After that, the viral ssRNA is released from the endosomal vesicle and then replicated in virus-induced membrane vesicles in the endoplasmic reticulum (ER). At the later stage of infection, vesicles containing immature virions are transported along the cellular secretory pathway and pass through the trans-Golgi network, where the host protease furin cleaves prM to generate mature virions that are secreted from the host cell (Yu et al. 2008). In our work, we found that a large number of proteins associated with intracellular membrane structure were regulated upon DENV infection. For example, we identified prolactin regulatory element binding protein (PREB) increased by ~ 1.5-fold upon DENV infection. PREB is a DNA-binding protein that specifically binds to a Pit1-binding element of the prolactin (PRL) promoter and then acts as a transcriptional regulator. PREB is mainly located in the ER (Fliss et al. 1999). It has been reported that PREB interacts with HCV NS4B and promotes HCV RNA replication (Kong et al. 2016).

On the basis of the GO analysis, cellular macromolecule biosynthetic process was identified as an overrepresented terminal processes in total regulated proteins. Lacking their own translational apparatus, viruses must recruit cellular ribosomes to translate viral mRNAs and produce the viral proteins for their replication. Here, we found several ribosomal proteins whose expression levels were regulated upon DENV infection, including RPS5, RPLP1, RPS27, RPL19, RPN1 and RSL1D1. In addition, several translational factors were also regulated, including EIF3E, EIF3J, EIF4A2, EIF5, EIF4EBP2, EEF1B2, EEF2K and TSFM.

These proteins are key factors in cellular protein biosynthesis, whose functions in DENV infection were not reported before. The above results suggest that DENV infection modulates host cellular protein biosynthesis at different levels and these proteins may function with nontraditional activities.

Another biological process is RNA splicing which is significantly enriched in total regulated proteins. RNA splicing is a form of RNA processing in which a newly made precursor messenger RNA (pre-mRNA) transcript is transformed into a mature messenger RNA (mRNA) by removing introns and joining exons together. Many viruses can utilize RNA splicing to facilitate the expression of their own genes and regulate the host gene expression. The protease 2A (2Apro) of poliovirus induces a selective nucleo-cytoplasm translocation of several important RNA binding/splicing proteins (Alvarez et al. 2013). In addition, previous studies reported that herpes simplex virus 1 (HSV-1) ICP27 protein inhibited the pre-mRNA splicing by interfering with host cellular splicing machinery (Lindberg & Kreivi, 2002; Sciabica et al. 2003). In our work, we found that the expression levels of several host proteins involved in RNA splicing is regulated upon DENV infection, including GTF2F2, POLR2C, SF3A3, SF3B3, DHX8, DHX16, PRPF40A, DNAJC8 and SRSF7. Future studies on these regulated proteins may help us uncover the novel mechanism(s) of DENV regulating the host RNA splicing process.

The eukaryotic genome is presented as a chromatin structure whose fundamental structure is the nucleosome. Therefore, chromatin structure and histone modifications play key roles in gene regulation. Recent studies indicate that several viral proteins can interact with host epigenetic factors. For example, HIV-1 integrase (IN) directly binds to SAP18 in vitro and in vivo. SAP18 and components of a Sin3A-HDAC1 complex were specifically incorporated into HIV-1. They also found HIV-1 virion-associated HDAC1 is required for efficient early post-entry events (Sorin et al. 2009). In our work, some epigenetic factors, such as SAP18, HDAC1, HMGN2, SETD2 and KDM38 were significantly regulated upon DENV infection, suggesting that DENV may regulate the host cell epigenetic program to facilitate virus replication.

Phosphorylation is the most typical PTM that involves the transfer of a phosphate group by a protein kinase to a target protein substrate on specific amino acids, such as serine (S), threonine (T), and tyrosine (Y). Phosphorylation regulates the signal transduction involved in many cellular biological processes by modulating protein activity and protein–protein interaction, altering protein structure, and controlling subcellular distribution. In our work, mRNA processing and regulation of transcription were identified as overrepresented terminal processes in phosphoproteins
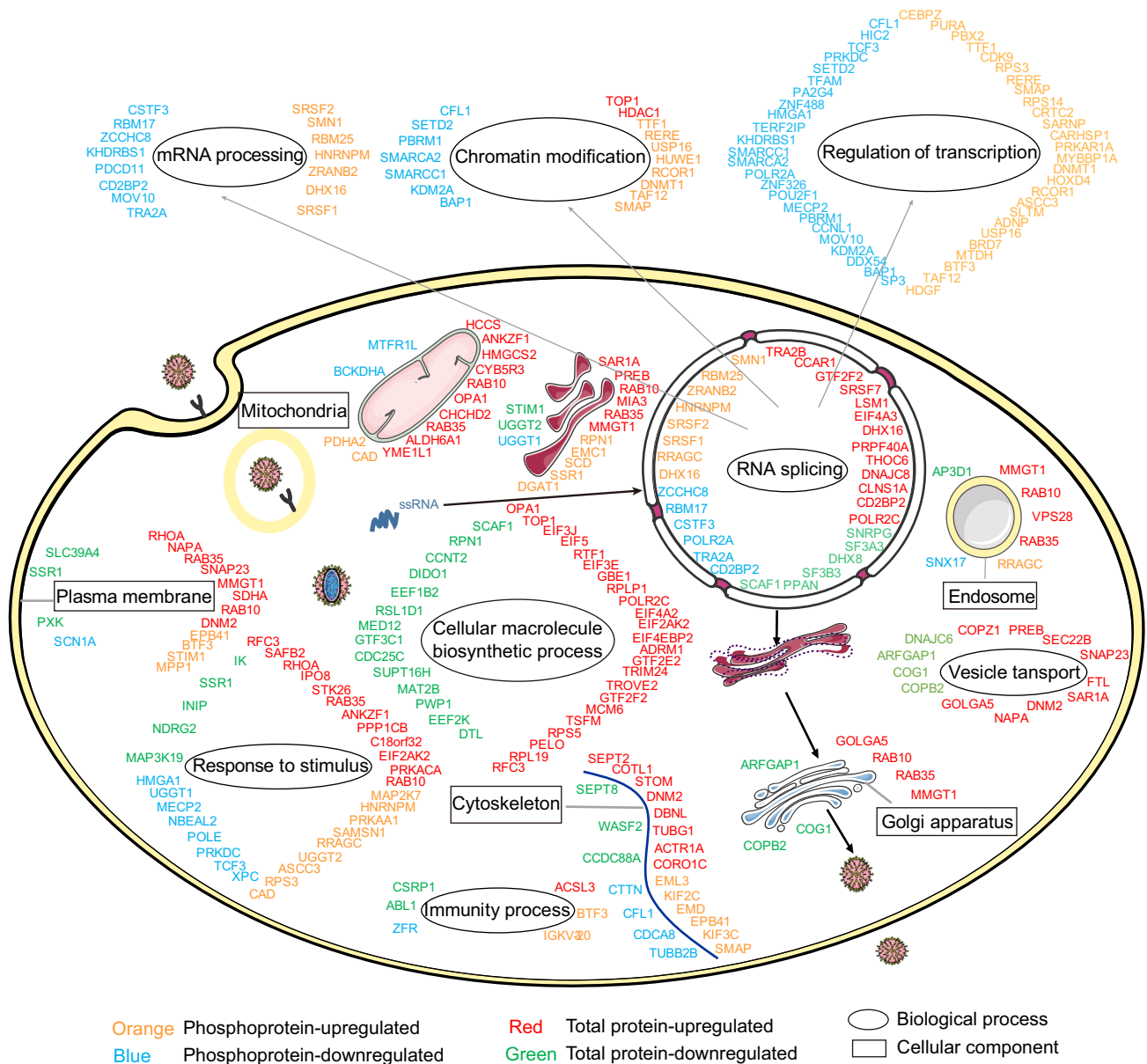
Fig. 5 Global view of total proteins and phosphoproteins regulation in K562 cells in response to DENV infection. The regulated total proteins and phosphoproteins were grouped in different categories according to cellular component or biological process which annotated by GO.

upon DENV infection. In mRNA processing, we found that the phosphorylation level of mobility group AT hook1 (HMGA1) protein was downregulated. Previous study showed that HMGA1 acts as a transcription factor responsible for the proinflammatory response upon the infection of highly pathogenic avian H5N1 virus (Viemann *et al.* 2011). Therefore, it is possible that the downregulated phosphorylation level of HMGA1 is associated with the response of host immune system to DENV infection. Moreover, our quantitative phosphoproteome analysis has revealed many cellular proteins and biological processes that are involved during DENV-2 virus infection. Most of the identified proteins have not been reported in

DENV infection before, and more studies will be needed in the future.

Recently, an interactome of DENV and host proteins was analyzed using affinity purification-mass spectrometry (AP-MS) (Shah *et al.* 2018). We compared our data with theirs and uncovered some overlapped proteins (Fig. 6, detailed information in Supplementary Table S8). Among these overlapped proteins, we noticed that MYBBP1A, PA2G4 and ZRANB2 also appeared in the network of mRNA processing and regulation of gene expression from regulated phosphoproteins. The phosphorylation levels of ZRANB2 and MYBBP1A were both upregulated, while PA2G4 was downregulated. Zinc finger Ran-binding
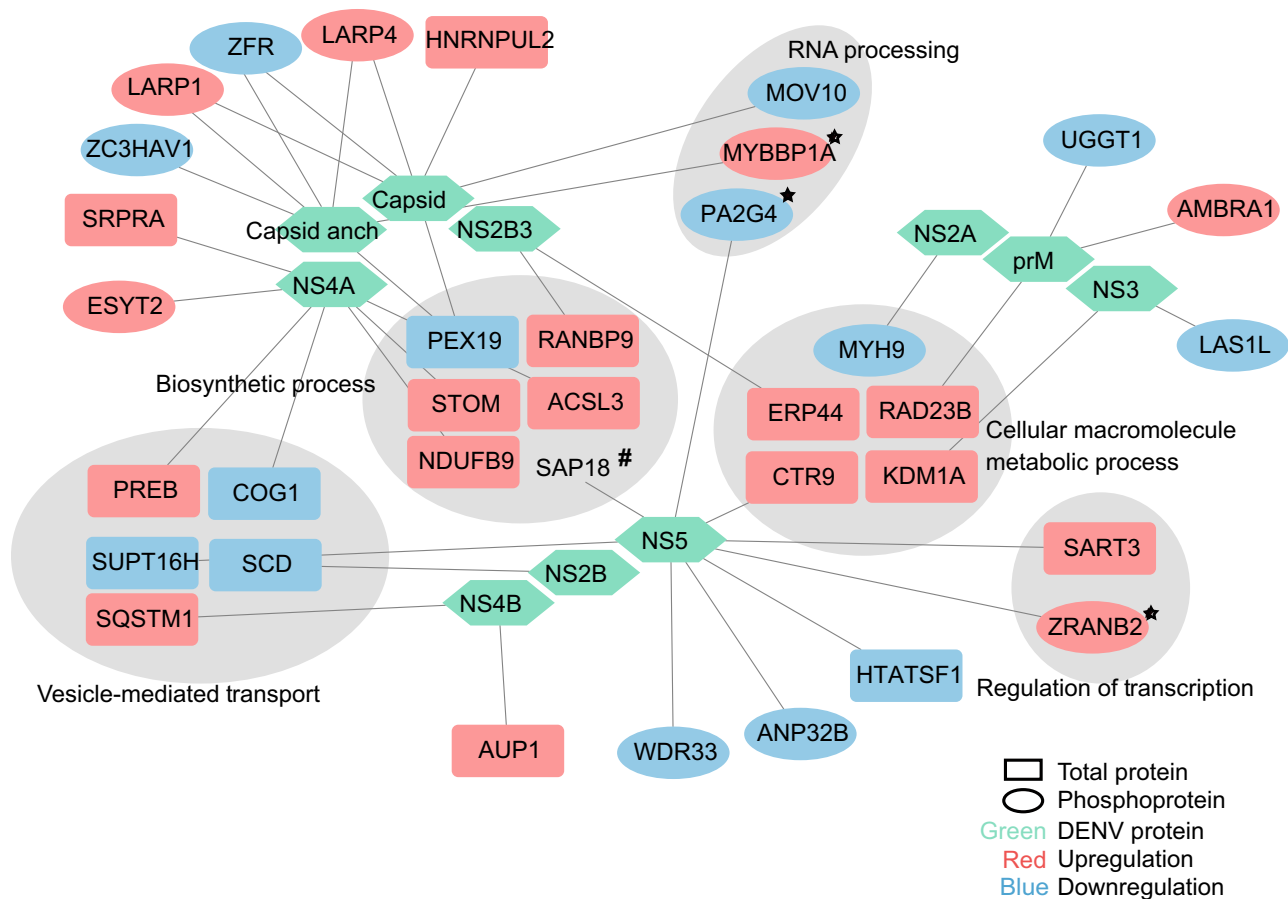
Fig. 6 Protein-protein interaction between Dengue proteins and significantly regulated proteins. Regulated protein and phosphoprotein data in this study were compared with host protein which interacted with DENV protein data in reference (note: Comparative Flavivirus-Host Protein Interaction Mapping Reveals Mechanisms of Dengue and Zika Virus Pathogenesis). 33 proteins overlapped in two studies. Gray region represents significant enriched processes in Fig. 3A, 3B. Star represent interacted proteins in Fig. 4A, 4C. Hash represent SAP18 identified in ZIKV AP-MS experiment.

domain-containing protein 2 (ZRANB2) can regulate alternative splicing and interact with several splicing proteins (Adams *et al.* 2001). ZRANB2 has been shown to bind mRNA, but modification of the ZRANB2 linker sequence will disturb the specific RNA binding capabilities.

Here, we found the phosphorylation level of ZRANB2 was upregulated after DENV infection and the interaction with NS5 was identified, suggesting its potential role in DENV infection. One work has showed that the nucleolar protein MYBB1A could associate with replicated viral DNA in order to reorganize its morphologies in the late phases of adenovirus replication (Komatsu *et al.* 2018). The upregulated phosphorylation level of MYBB1A and its interaction with capsid protein may imply its role in DENV replication. Proliferation-associated protein 2G4 (PA2G4) regulates cell proliferation, differentiation and cap-independent translation of specific viral IRESs (Liu *et al.* 2006; Squatrito *et al.* 2004). Phosphorylation at Ser-361 regulates

its nucleolar localization. It has been reported that PA2G4 was significantly down-regulated in cells transfected with HIV-1 Vpr (Zhang *et al.* 2014). We found that the phosphorylation level of PA2G4 is downregulated, along with its ability to interact with NS5, which may reveal its new function in dengue virus replication.

We also compared our work with other previous studies. Pando-Robles *et al.* have reported 155 cellular proteins were regulated in DENV-infected Huh-7 cells by using label-free LC–MS (Pando-Robles *et al.* 2014). Three proteins EFHD2, GPS1 and EIF2AK2 were also observed as regulated in our results. Another study of DENV infected A549 cells was analyzed by SILAC and mass spectrometry (Chiu *et al.* 2014), three up-regulated proteins ECI2, SDF2L1 and EEF1A2 and four downregulated proteins SCD, PWP1, DHX8 and MED12 were also detected in our study. As for flaviviruses JEV and ZIKV, four regulated proteins GPS1, EIF2AK2, HMGCS1 and RPN1 in JEV infected Hela cells and two proteins DPH5 and GTF2E2 in

ZIKV infected C6/36 cells (Xin *et al.* 2017; Zhang *et al.* 2013) were also observed in our study.

In summary, this study systematically identified a number of host cellular proteins and phosphoproteins that were differentially regulated in response to DENV infection. Most of these proteins were involved in transcription regulation, RNA splicing and processing, immune system, cellular response to stimulus and macromolecule biosynthesis. Potential roles of several altered proteins as host responses to DENV were discussed, which could be related to cellular antiviral response or pathogenic mechanisms. Further investigations are needed to elucidate the functional significance of the other proteins with altered expression or modification. The present study provides comprehensive information of protein expression and phosphorylation, which is valuable for understanding the interplay between host and DENV.

Author contributions XLZ and XZ designed the research; XLZ, MM, FY, DYW and JYX performed the research; XLZ, XZ, MM, FY, YJT and LTY analyzed the data; XLZ, MM and FY drafted the paper; XLZ, XZ and YQ revised the paper.

Compliance with ethical standards

Conflict of interest The authors declare no competing interests.

Animal and Human Rights Statement This article does not contain any studies with human or animal subjects performed by any of the authors.

References

Acosta EG, Castilla V, Damonte EB (2008) Functional entry of dengue virus into aedes albopictus mosquito cells is dependent on clathrin-mediated endocytosis. J Gen Virol 89:474–484

Adams DJ, van der Weyden L, Mayeda A, Stamm S, Morris BJ, Rasko JE (2001) Znf265—a novel spliceosomal protein able to induce alternative splicing. J Cell Biol 154:25–32

Aguirre S, Maestre AM, Pagni S, Patel JR, Savage T, Gutman D, Maringer K, Bernal-Rubio D, Shabman RS, Simon V, Rodriguez-Madoz JR, Mulder LC, Barber GN, Fernandez-Sesma A (2012) DENV inhibits type i IFN production in infected cells by cleaving human sting. PLoS Pathog 8:e1002934

Alvarez E, Castello A, Carrasco L, Izquierdo JM (2013) Poliovirus 2a protease triggers a selective nucleo-cytoplasmic redistribution of splicing factors to regulate alternative pre-mrna splicing. PLoS ONE 8:e73723

Bhatt S, Gething PW, Brady OJ, Messina JP, Farlow AW, Moyes CL, Drake JM, Brownstein JS, Hoen AG, Sankoh O, Myers MF, George DB, Jaenisch T, Wint GR, Simmons CP, Scott TW, Farrar JJ, Hay SI (2013) The global distribution and burden of dengue. Nature 496:504–507

Boersema PJ, Raijmakers R, Lemeer S, Mohammed S, Heck AJ (2009) Multiplex peptide stable isotope dimethyl labeling for quantitative proteomics. Nat Protoc 4:484–494

Chiu HC, Hannemann H, Heesom KJ, Matthews DA, Davidson AD (2014) High-throughput quantitative proteomic analysis of dengue virus type 2 infected a549 cells. PLoS ONE 9:e93305

Clements DR, Murphy JP, Sterea A, Kennedy BE, Kim Y, Helson E, Almasi S, Holay N, Konda P, Paulo JA, Sharif T, Lee PW, Weekes MP, Gygi SP, Gujar S (2017) Quantitative temporal in vivo proteomics deciphers the transition of virus-driven myeloid cells into m2 macrophages. J Proteome Res 16:3391–3406

Daffis S, Szretter KJ, Schriewer J, Li J, Youn S, Errett J, Lin TY, Schneller S, Zust R, Dong H, Thiel V, Sen GC, Fensterl V, Klimstra WB, Pierson TC, Buller RM, Gale M Jr, Shi PY, Diamond MS (2010) 2′-o methylation of the viral mrna cap evades host restriction by ifit family members. Nature 468:452–456

Ersing I, Nobre L, Wang LW, Soday L, Ma Y, Paulo JA, Narita Y, Ashbaugh CW, Jiang C, Grayson NE, Kieff E, Gygi SP, Weekes MP, Gewurz BE (2017) A temporal proteomic map of epstein-barr virus lytic replication in b cells. Cell Rep 19:1479–1493

Fliss MS, Hinkle PM, Bancroft C (1999) Expression cloning and characterization of preb (prolactin regulatory element binding), a novel wd motif DNA-binding protein with a capacity to regulate prolactin promoter activity. Mol Endocrinol 13:644–657

Green AM, Beatty PR, Hadjilaou A, Harris E (2014) Innate immunity to dengue virus infection and subversion of antiviral responses. J Mol Biol 426:1148–1160

Hsu JL, Chen SH (2016) Stable isotope dimethyl labelling for quantitative proteomics and beyond. Philos Trans A Math Phys Eng Sci 374:20150364

Huynh VT, Lim YS, Tran SC, Pham TM, Nguyen LN, Hwang SB (2016) Hepatitis c virus nonstructural 5a protein interacts with abelson interactor 1 and modulates epidermal growth factor-mediated mek/erk signaling pathway. J Biol Chem 291:22607–22617

Komatsu T, Quentin-Froignant C, Carlon-Andres I, Lagadec F, Rayne F, Ragues J, Kehlenbach RH, Zhang W, Ehrhardt A, Bystricky K, Morin R, Lagarde JM, Gallardo F, Wodrich H (2018) In vivo labelling of adenovirus DNA identifies chromatin anchoring and biphasic genome replication. J Virol 92:e00795-18

Kong L, Fujimoto A, Nakamura M, Aoyagi H, Matsuda M, Watashi K, Suzuki R, Arita M, Yamagoe S, Dohmae N, Suzuki T, Sakamaki Y, Ichinose S, Suzuki T, Wakita T, Aizaki H (2016) Prolactin regulatory element binding protein is involved in hepatitis c virus replication by interaction with ns4b. J Virol 90:3093–3111

Li G, Pan P, He Q, Kong X, Wu K, Zhang W, Liu Y, Huang H, Liu J, Zhang Z, Wu, Lai X, Liu X, Wu J (2017) Molecular epidemiology demonstrates that imported and local strains circulated during the 2014 dengue outbreak in Guangzhou, China. Virol Sin 32:63–72

Lindberg A, Kreivi JP (2002) Splicing inhibition at the level of spliceosome assembly in the presence of herpes simplex virus protein icp27. Virology 294:189–198

Liu Z, Ahn JY, Liu X, Ye K (2006) Ebp1 isoforms distinctively regulate cell survival and differentiation. Proc Natl Acad Sci U S A 103:10917–10922

Liu X, Wang X, Wang Q, Luo M, Guo H, Gong W, Tu C, Sun J (2018) The eukaryotic translation initiation factor 3 subunit e

binds to classical swine fever virus ns5a and facilitates viral replication. Virology 515:11–20

Maere S, Heymans K, Kuiper M (2005) Bingo: a cytoscape plugin to assess overrepresentation of gene ontology categories in biological networks. Bioinformatics 21:3448–3449

Masutani M, Sonenberg N, Yokoyama S, Imataka H (2007) Reconstitution reveals the functional core of mammalian eIF3. EMBO J 26:3373–3383

Messina JP, Brady OJ, Scott TW, Zou C, Pigott DM, Duda KA, Bhatt S, Katzelnick L, Howes RE, Battle KE, Simmons CP, Hay SI (2014) Global spread of dengue virus types: mapping the 70 year history. Trends Microbiol 22:138–146

Mi H, Huang X, Muruganujan A, Tang H, Mills C, Kang D, Thomas PD (2017) Panther version 11: expanded annotation data from gene ontology and reactome pathways, and data analysis tool enhancements. Nucleic Acids Res 45:D183–D189

Pando-Robles V, Oses-Prieto JA, Rodriguez-Gandarilla M, Meneses-Romero E, Burlingame AL, Batista CV (2014) Quantitative proteomic analysis of huh-7 cells infected with dengue virus by label-free LC-MS. J Proteomics 111:16–29

Radke EG, Gregory CJ, Kintziger KW, Sauber-Schatz EK, Hunsperger EA, Gallagher GR, Barber JM, Biggerstaff BJ, Stanek DR, Tomashek KM, Blackmore CG (2012) Dengue outbreak in key west, florida, USA, 2009. Emerg Infect Dis 18:135–137

Savidis G, McDougall WM, Meraner P, Perreira JM, Portmann JM, Trincucci G, John SP, Aker AM, Renzette N, Robbins DR, Guo Z, Green S, Kowalik TF, Brass AL (2016) Identification of zika virus and dengue virus dependency factors using functional genomics. Cell Rep 16:232–246

Schaffner F, Fontenille D, Mathis A (2014) Autochthonous dengue emphasises the threat of arbovirosis in europe. Lancet Infect Dis 14:1044

Schubert OT, Rost HL, Collins BC, Rosenberger G, Aebersold R (2017) Quantitative proteomics: challenges and opportunities in basic and applied research. Nat Protoc 12:1289–1294

Sciabica KS, Dai QJ, Sandri-Goldin RM (2003) Icp27 interacts with srpk1 to mediate hsv splicing inhibition by altering sr protein phosphorylation. EMBO J 22:1608–1619

Shah PS, Link N, Jang GM, Sharp PP, Zhu T, Swaney DL, Johnson JR, Von Dollen J, Ramage HR, Satkamp L, Newton B, Huttenhain R, Petit MJ, Baum T, Everitt A, Laufman O, Tassetto M, Shales M, Stevenson E, Iglesias GN, Shokat L, Tripathi S, Balasubramaniam V, Webb LG, Aguirre S, Willsey AJ, Garcia-Sastre A, Pollard KS, Cherry S, Gamarnik AV, Marazzi I, Taunton J, Fernandez-Sesma A, Bellen HJ, Andino R, Krogan NJ (2018) Comparative flavivirus-host protein interaction mapping reveals mechanisms of dengue and zika virus pathogenesis. Cell 175:1931–1945.e1918

Shannon P, Markiel A, Ozier O, Baliga NS, Wang JT, Ramage D, Amin N, Schwikowski B, Ideker T (2003) Cytoscape: a software environment for integrated models of biomolecular interaction networks. Genome Res 13:2498–2504

Simmons CP, Farrar JJ, Nguyen v V, Wills B (2012) Dengue. N Engl J Med 366:1423–1432

Singh KK, Erkelenz S, Rattay S, Dehof AK, Hildebrandt A, Schulze-Osthoff K, Schaal H, Schwerk C (2010) Human sap18 mediates assembly of a splicing regulatory multiprotein complex via its ubiquitin-like fold. RNA 16:2442–2454

Sorin M, Cano J, Das S, Mathew S, Wu X, Davies KP, Shi X, Cheng SW, Ott D, Kalpana GV (2009) Recruitment of a sap18-hdac1

complex into hiv-1 virions and its requirement for viral replication. PLoS Pathog 5:e1000463

Squatrito M, Mancino M, Donzelli M, Areces LB, Draetta GF (2004) Ebp1 is a nucleolar growth-regulating protein that is part of pre-ribosomal ribonucleoprotein complexes. Oncogene 23:4454–4465

Szklarczyk D, Morris JH, Cook H, Kuhn M, Wyder S, Simonovic M, Santos A, Doncheva NT, Roth A, Bork P, Jensen LJ, von Mering C (2017) The string database in 2017: quality-controlled protein-protein association networks, made broadly accessible. Nucleic Acids Res 45:D362–D368

Thongtan T, Panyim S, Smith DR (2004) Apoptosis in dengue virus infected liver cell lines hepg2 and hep3b. J Med Virol 72:436–444

Viemann D, Schmolke M, Lueken A, Boergeling Y, Friesenhagen J, Wittkowski H, Ludwig S, Roth J (2011) H5n1 virus activates signaling pathways in human endothelial cells resulting in a specific imbalanced inflammatory response. J Immunol 186:164–173

Wang K, Yin XM, Chao DT, Milliman CL, Korsmeyer SJ (1996) Bid: a novel bh3 domain-only death agonist. Genes Dev 10:2859–2869

Weekes MP, Tomasec P, Huttlin EL, Fielding CA, Nusinow D, Stanton RJ, Wang EC, Aicheler R, Murrell I, Wilkinson GW, Lehner PJ, Gygi SP (2014) Quantitative temporal viromics: an approach to investigate host-pathogen interaction. Cell 157:1460–1472

Welsch S, Miller S, Romero-Brey I, Merz A, Bleck CK, Walther P, Fuller SD, Antony C, Krijnse-Locker J, Bartenschlager R (2009) Composition and three-dimensional architecture of the dengue virus replication and assembly sites. Cell Host Microbe 5:365–375

World Health Organization (WHO) Dengue and severe dengue. https://www.who.int/en/news-room/fact-sheets/detail/dengue-and-severe-dengue. Accessed 15 Apr 2019

Xin QL, Deng CL, Chen X, Wang J, Wang SB, Wang W, Deng F, Zhang B, Xiao G, Zhang LK (2017) Quantitative proteomic analysis of mosquito C6/36 cells reveals host proteins involved in zika virus infection. J Virol 91:e00554-17

Yu IM, Zhang W, Holdaway HA, Li L, Kostyuchenko VA, Chipman PR, Kuhn RJ, Rossmann MG, Chen J (2008) Structure of the immature dengue virus at low ph primes proteolytic maturation. Science 319:1834–1837

Zhang Y, Iratni R, Erdjument-Bromage H, Tempst P, Reinberg D (1997) Histone deacetylases and sap18, a novel polypeptide, are components of a human sin3 complex. Cell 89:357–364

Zhang LK, Chai F, Li HY, Xiao G, Guo L (2013) Identification of host proteins involved in japanese encephalitis virus infection by quantitative proteomics analysis. J Proteome Res 12:2666–2678

Zhang S, Zhang B, Xu X, Wang L, Feng X, Wang Q, Huang H, Wu J, Li P, Wang J (2014) Hiv-1 viral protein r downregulates Ebp1 and stabilizes p53 in glioblastoma U87MG cells. Clin Transl Oncol 16:293–300

Zhao X, Bak S, Pedersen AJ, Jensen ON, Hojlund K (2014) Insulin increases phosphorylation of mitochondrial proteins in human skeletal muscle in vivo. J Proteome Res 13:2359–2369

Zhao H, Zhang FC, Zhu Q, Wang J, Hong WX, Zhao LZ, Deng YQ, Qiu S, Zhang Y, Cai WP, Cao WC, Qin CF (2016) Epidemiological and virological characterizations of the 2014 dengue outbreak in Guangzhou, China. PLOS One 11:e156548